

In situ spectroscopic identification of the six types of asbestos

Vladimir Zholobenko ^{a}, Frank Rutten ^{a,b}, Aleksey Zholobenko ^c, Amy Holmes ^a*

^a *School of Chemical and Physical Sciences, Keele University, Keele, ST5 5BG, United Kingdom*

^b *ATBC, HAN University of Applied Sciences, 6525 EM Nijmegen, The Netherlands*

^c *Larchwood, Newcastle-under-Lyme, ST5 5BB, United Kingdom*

Abstract

Exposure to asbestos fibres is related to a number of severe lung diseases, and therefore, rapid, accurate and reliable in situ or on-site asbestos detection in real-life samples is of considerable importance. This work presents a comprehensive investigation of all six types of asbestos by mid-infrared ATR-FTIR, NIR spectroscopy and Raman microspectroscopy. Our studies demonstrate that for practical applications, NIR spectroscopy is potentially the most powerful method for asbestos identification in materials utilised by the construction industry. By focusing on the narrow spectral region, 7300-7000 cm⁻¹ (~1370-1430 nm, overtones of O-H vibrations), which is highly specific to these materials, and optimising the sensitivity and resolution of the instrumentation, we have been able to discriminate and identify each of the six types of asbestos with the level of detection significantly better than 1 wt%. Furthermore, straightforward computational analysis has allowed for automated objective evaluation of the spectroscopic data.

Keywords: asbestos containing materials; mid-IR spectroscopy; Raman spectroscopy; NIR spectroscopy

* Corresponding author
e-mail address: v.l.zholobenko@keele.ac.uk

32 ***Introduction***

33 Asbestos is a generic term for a group of six silicate minerals (chrysotile, amosite,
34 crocidolite, actinolite, tremolite and anthophyllite), from the serpentine and amphibole groups,
35 which possess an asbestiform fibrous morphology. The amphibole type asbestos materials (all
36 except chrysotile) have a chemical composition $M_7Si_8O_{22}(OH)_2$, where M stands for metal
37 cations, such as calcium, iron, magnesium or sodium. Chrysotile, a serpentine mineral, has a
38 distinctive $Mg_3Si_2O_5(OH)_4$ composition [1,2]. Asbestos has been widely utilised in industry
39 owing to its valuable properties, including high tensile strength, heat and fire resistance,
40 electrical resistance and chemical inertness. Chrysotile accounts for around 95% of naturally
41 occurring asbestos, and hence has been most commonly employed on the industrial scale.
42 Crocidolite and amosite were also widely used. Applications of these materials include brake
43 shoes and gaskets, insulation board, cement, fire blankets, corrugated roofing tiles, membranes
44 for chlorine production and many others [3,4,5,6,7,8]. In many countries, the use of asbestos is
45 now restricted or banned due to the severe health risks it poses. The structural and chemical
46 properties of the fibres inhaled into the lungs lead to severe tissue damage causing asbestosis,
47 mesothelioma and other pleural diseases [9,10]. Considering the high potential risks resulting
48 from the contact with asbestos containing materials (ACM), it is important to be able to
49 efficiently and reliably detect them.

50 The current standard methods for asbestos identification are polarised light microscopy
51 (PLM) for bulk samples, and phase contrast microscopy (PCM) for airborne fibres. In PLM, the
52 optical properties of a solid sample, including pleochroism, refractive index and birefringence,
53 are observed under plane polarised and cross polarised light. In PCM, a volume of air is passed
54 through a filter and then the concentration of fibres is determined. PCM is less specific than
55 PLM as very limited characterisation is carried out [5,11,12]. Limitations of PLM include the
56 subjective nature of analysis, and its inability to provide quantitative information on the structure
57 or chemical composition of the examined fibres. Other analytical techniques which could
58 overcome some of these limitations include x-ray diffraction, electron microscopy and
59 vibrational spectroscopy [12,13].

60 Studies of asbestos using vibrational spectroscopy began in the 1970s, and have been
61 discussed in the literature since. The research documented has largely focused on collecting
62 infrared and Raman spectra of asbestos minerals in order to determine the relationship between
63 spectral bands and structural features [14,15,16,17,18,19]. The aim of this work is to explore the
64 effectiveness of mid-IR, NIR and Raman spectroscopy for the everyday detection of asbestos
65 in suspected ACM, particularly materials utilised in the construction industry. The challenge is to
66 apply these techniques to the detection of asbestos in a wide range of possible organic and
67 inorganic matrices which can interfere with the analysis, from bitumen and structural paints to

68 cement and plasterboards. The examined ACM may be presented as powdered, fibrous or
69 compacted solid materials, which should be tested with minimal sample preparation.
70 Furthermore, environmental, and health and safety agencies generally require to identify each of
71 the six types of asbestos even when its concentration is below 1 wt%. The emphasis of our
72 investigation is on the practical application of spectroscopic techniques for the reliable analysis
73 of real-world materials, possibly on-site or in situ, that is to achieve identification of every type
74 of asbestos present in a sample as a major constituent or in trace quantities. Spectra of reference
75 asbestos samples, potential replacement fibres and matrix materials, and real-life ACM have
76 been collected with virtually no sample preparation. The data have been analysed using a number
77 of computational approaches, and the advantages and limitations of each spectroscopic technique
78 are discussed. (The Supplementary Information files provide a comprehensive description of the
79 experimental procedures.) The results of these investigations, which have been correlated with
80 the PLM data, demonstrate that NIR spectroscopy is conceivably the most powerful technique
81 for routine practical detection and identification of asbestos. Our work shows that NIR is a more
82 viable option than Raman microscopy and ATR-FTIR for in situ screening of ACM samples,
83 which is largely due to its greater penetration depth. Therefore, a dedicated computational
84 analysis protocol is developed specifically for the evaluation of NIR data.

85

86 ***Experimental***

87 To ensure safe working practices, all experiments were carried out using a negative-
88 pressure ventilated safety box with an extraction system equipped with a H-type filter.

89 *Materials.* The reference samples characterised using FTIR and Raman spectroscopy are
90 shown in Table S1. The samples were divided into two groups, geological asbestos reference
91 samples (provided by the Health and Safety Laboratories, UK, and Geology department at Keele
92 University) and non-asbestos matrix materials (sourced locally). ACM samples with unknown
93 asbestos content were supplied by Greenwall Environmental and accompanied with the PLM
94 analysis data. The original samples, including fibrous (reference asbestos and asbestos rope),
95 powdered (cement and dry textured coating) and compacted solid (tiles and blocks) materials
96 were analysed as received without any pretreatment, enrichment or fibre extraction. Typically, a
97 sample, with the size of 10x10x5 mm, was fixed onto a sample holder of the relevant
98 spectrometer and characterised using one of the vibrational spectroscopy techniques.

99 *Vibrational Spectroscopy.* FTIR spectra were collected using Thermo Nicolet Avatar 320
100 and iS10 FTIR spectrometers equipped with DTGS detectors and attenuated total reflectance
101 (ATR) attachments. Two ATR attachments, with a diamond coated zinc selenide crystal and a
102 diamond crystal, were used in order to ensure minimal sample preparation. The spectra were
103 collected using 4 cm⁻¹ resolution, 64-128 scans (~130 to 260 seconds data collection time;

104 sampling spot size ~2 by 2 mm), 4000-550 cm^{-1} range for the diamond coated zinc selenide ATR
105 and 4000-400 cm^{-1} range for the diamond ATR. The Raman spectra were obtained using a
106 Thermo Scientific DXR microscope, which is a dispersive instrument with interchangeable
107 lasers and optical elements working with 780 nm and 532 nm excitation wavelengths. The
108 typical parameters for the data collection were: 4 cm^{-1} resolution, 0.1-0.5 second exposure time,
109 200-2000 scans (~20 to 1000 seconds data collection time; sampling spot size ~10 to 50 μm), 10-
110 24 mW laser power and a spectral range of 3300-40 cm^{-1} . NIR spectra were collected using a
111 Thermo Antaris II spectrometer equipped with an InGaAs detector and a diffuse reflectance
112 attachment. The spectra collection parameters were: 2-32 cm^{-1} resolution, 16-128 scans (~5 to
113 100 seconds data collection time) and 10000-4000 cm^{-1} spectral range.

114 *Data Analysis.* The analysis of vibrational spectra, including band search, intensity
115 measurements and a multi-component search, was carried out using Omnic and Specta software
116 (Thermo Scientific). For the spectra shown, no smoothing was applied; however, some spectra
117 are offset along the y-axis for the clarity of presentation.

118 NIR spectra were analysed using our own basic computational tool Asbestos-Tester-4-v-
119 0.1.0. The program's source code was written in the Rust programming language and compiled
120 with the 1.33.0-nightly tool-chain. The computational algorithm was designed for the analysis of
121 NIR spectra obtained at a resolution of 4 cm^{-1} , in the region of 7300-7000 cm^{-1} , saved as csv files.
122 The data analysis relies on the comparison between the NIR spectra of unknown samples and the
123 reference spectra of asbestos, taking into account the band positions and intensities. The program
124 was evaluated using 50 samples, including reference materials, and 9 data sets for each sample.
125 The 9 data sets were obtained by collecting NIR spectra in 3 different locations for every sample,
126 3 times in each location. The results, computed for every data set, indicated the presence or
127 absence of different types of asbestos. The program examined each spectrum for the presence of
128 each type of asbestos. The current version of Asbestos-Tester-4 was compiled to test for the
129 presence of four more common types of asbestos: chrysotile, actinolite, amosite and crocidolite.
130 The number of reference asbestos types and the data analysis parameters can be easily changed
131 by a competent user. This program is made freely available for not-for-profit use as part of this
132 publication. The source code can be found at <https://github.com/aleshaleksey/asbestos-test/>.

133
134

135 ***Results and Discussion***

136 *ATR-FTIR characterisation.* All six types of asbestos reference samples have been
137 studied (Table S1), and Figures 1 and S1 show characteristic spectra of these materials
138 exemplifying the key bands observed; their positions and assignment are summarised in Table
139 S2. Two regions in the spectra are of particular interest: the 3700-3500 cm⁻¹ region can be
140 attributed to O-H stretching vibrations, whereas the bands observed in the 1200-500 cm⁻¹ region
141 can be ascribed to various lattice vibrations [15,20,21]. The mid-IR spectra demonstrate
142 significant reproducible differences between all types of asbestos, and therefore, FTIR data could
143 be used to distinguish asbestos samples by applying statistical techniques and computerised
144 search of reference libraries. Within the scope of this study, a number of reference materials have
145 been chosen that are likely to be present alongside asbestos, including matrix materials and
146 asbestos replacement fibres, e.g. polyamide or glass fibres. FTIR spectra of such fibres are
147 shown in Figure S2. Since the majority of the distinctive bands in the asbestos spectra are in the
148 same region (1200-900 cm⁻¹) as the intense bands in the spectra of silica-based inorganic fibres,
149 their presence in a material could impede the detection of asbestos. In contrast, the bands
150 observed in the spectra of organic fibres are found predominantly in different regions, hence, the
151 presence of most organic fibres is unlikely to affect asbestos detection. Figure S3 shows FTIR
152 spectra of three common matrix materials: bitumen, cement and plasterboard, all of which
153 contain bands, for instance in the 1300-500 cm⁻¹ region, that may overlap with the asbestos
154 bands in unknown ACM materials.

155

156

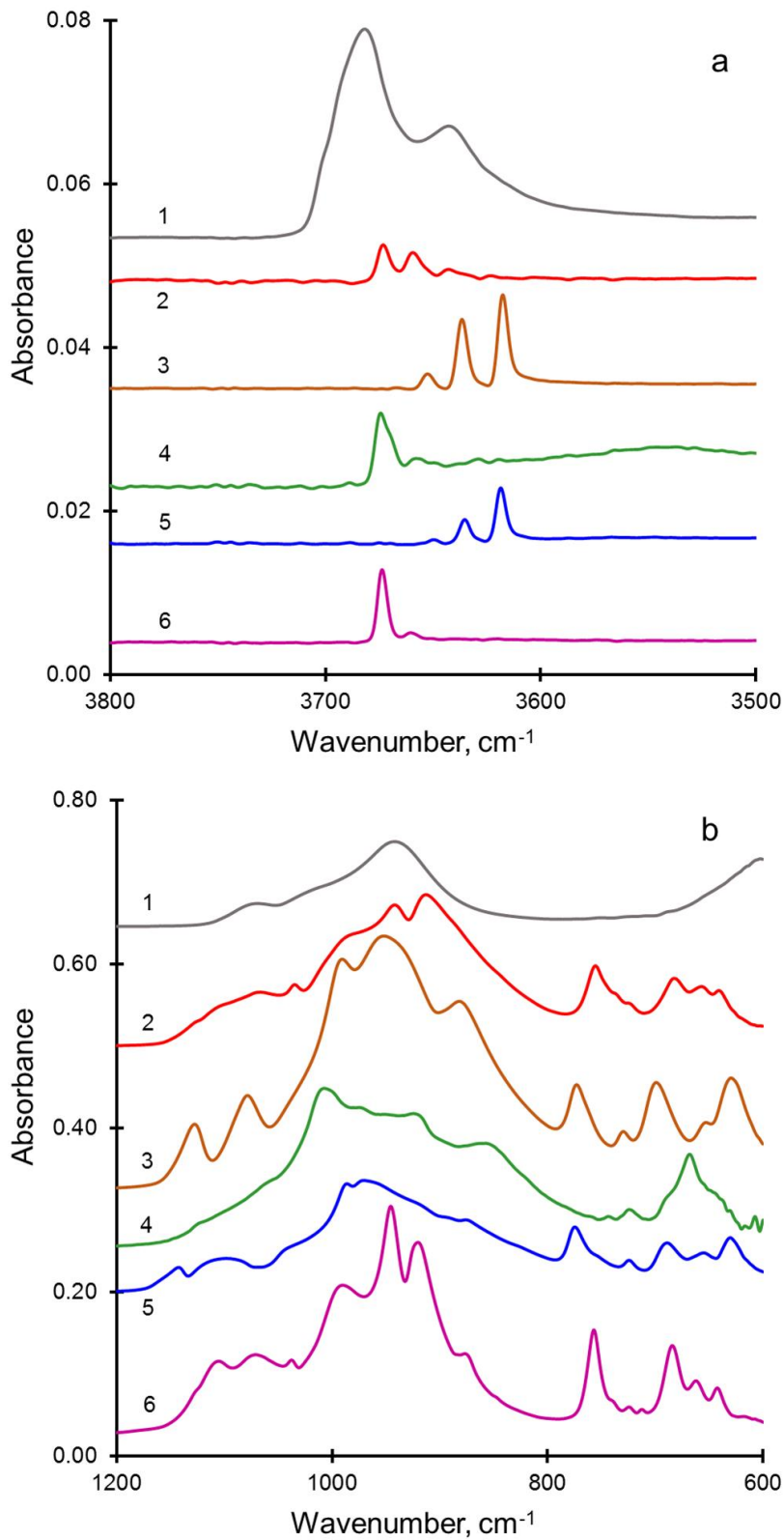


Figure 1. FTIR spectra of reference asbestos samples: (a) region of O-H stretching vibrations and (b) region of structural vibrations. Note ~10-fold difference in the absorbance scale. (1) δ chrysotile, (2) δ actinolite, (3) δ amosite, (4) δ anthophyllite, (5) δ crocidolite, (6) δ tremolite (resolution = 4 cm⁻¹).

158 A range of suspected ACM have been characterised by PLM and FTIR aiming to
159 determine which type of asbestos may be present in each sample. The FTIR spectra of 43
160 samples have been initially analysed by comparing the band positions with those observed for
161 the reference materials (Figure S4). In addition, specialised software Spectra has been tested for
162 the identification of individual components in ACM to match the unknown spectrum, utilising a
163 multi-component search and producing a composite spectrum from the relevant library spectra.
164 The simulated spectrum is rated in comparison to the spectrum of the examined sample using the
165 proprietary match and composite values, which quantify how well the two spectra match and the
166 percentage contribution of each reference spectrum to the composite spectrum (see Figures S5
167 and S6, and related discussion). The results obtained are in good agreement with those
168 subsequently provided by PLM for 34 out of 43 ACM samples (Table S3), however, omissions
169 in the spectral libraries can lead to very low match values for some samples. Indeed, for some
170 ACM the data are inconclusive, particularly, when the asbestos percentage contribution to the
171 composite spectrum is below 5%. Overall, ATR-FTIR spectroscopy can be successfully utilised
172 for the analysis of ACM with a high asbestos concentration (estimated as above 20 wt%).
173 Nonetheless, the low sampling depth typical of mid-infrared spectroscopy (a few microns), and
174 the presence of interfering IR bands, owing to the vast range of matrix materials, can severely
175 compromise the analytical power of this technique for the real-life asbestos identification.
176 Moreover, the use of ATR requires direct contact with the sample, which in turn necessitates
177 additional safety measures to prevent potential asbestos exposure.

178 *Raman Spectroscopy.* In general, Raman spectroscopy is a highly sensitive analytical tool
179 widely used for structural characterisation and identification of pharmaceuticals, polymers and
180 other materials. Spectra of the reference asbestos samples and a selection of ACM have been
181 collected to determine the utility of this technique for asbestos identification (Figures 2, S7 and
182 S8, and Table S4). Although this is probably the first reported study of all six types of asbestos
183 using two different excitation wavelengths in the visible and NIR regions, which can therefore
184 serve as a reference source, the effectiveness of Raman spectroscopy for the analysis of real-life
185 ACM has not been satisfactory. A number of ACM samples and a range of sampling conditions
186 have been tested, but in all cases the signal to noise ratio is low, the background from any non-
187 asbestos constituent is significant and the spectral contribution from the matrix materials is rather
188 high. While the spectra collected using different excitation wavelengths have yielded a better
189 signal to noise ratio and decreased background for some samples, the identification of asbestos in
190 real-life ACM using Raman spectroscopy has been unsatisfactory [16,17]. Furthermore,
191 according to [20,22,23,24], Raman spectra of asbestos minerals and their non-fibrous analogues
192 (chrysotile and lizardite, amosite and grunerite, crocidolite and riebeckite) are quite similar,
193 making their identification even more challenging.

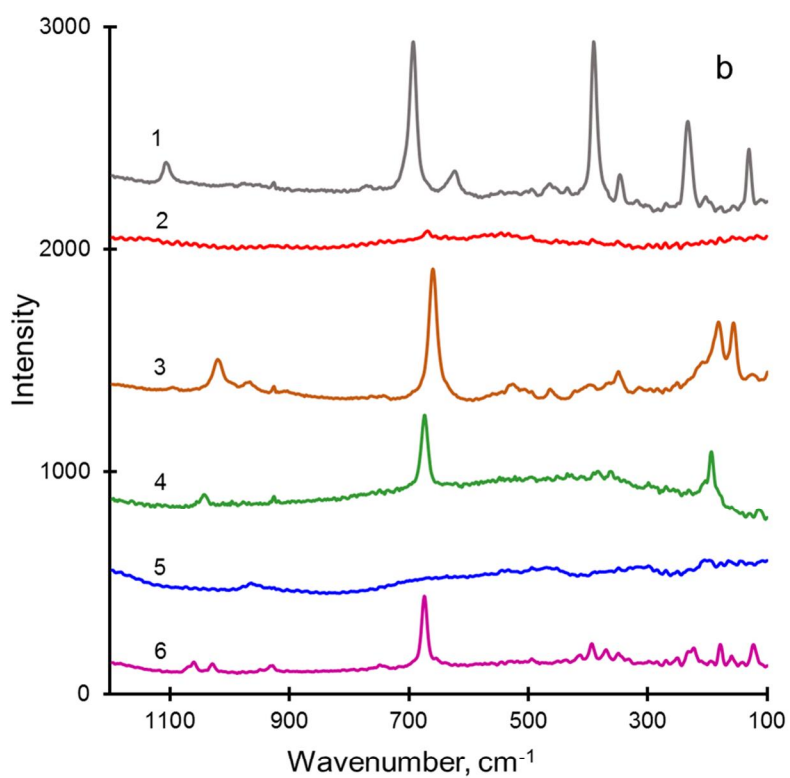
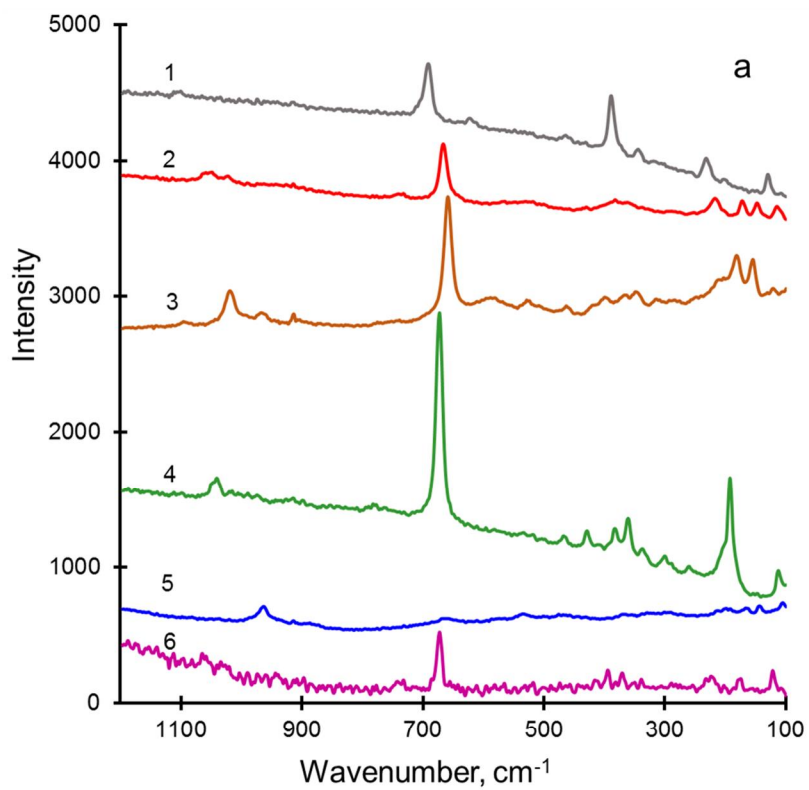


Figure 2. Raman spectra of asbestos reference samples collected using (a) 532 nm and (b) 780 nm excitation wavelength: (1) δ chrysotile, (2) δ actinolite, (3) δ amosite, (4) δ anthophyllite, (5) δ crocidolite, (6) δ tremolite (resolution = 4 cm^{-1}).

195 *Near-infrared spectroscopy*. NIR has a wide range of applications in polymer,
196 pharmaceutical and food industries. It is particularly useful for the identification and
197 quantification of a known compound within a well understood mixture or matrix [25]. As stated
198 previously, it is essential to achieve successful detection of asbestos in a wide range of unknown
199 matrices and to identify each of the six types of asbestos even when its concentration is below 1
200 wt%. NIR spectra of six types of asbestos and those for a selection of matrix materials, collected
201 at a relatively high resolution (2 cm^{-1}) in the region $7300\text{-}7000\text{ cm}^{-1}$, are presented in Figures 3,
202 S9 and S10. The observed bands, corresponding to the first overtone of the O-H stretching
203 vibrations, show a distinctive pattern for each type of asbestos as compared to any organic or
204 inorganic material examined in this work, including minerals of similar composition (e.g. non-
205 fibrous tremolite, brucite and mica). For potential practical applications, it is important to note
206 that the same high quality spectra have been obtained for asbestos samples analysed through a
207 plastic bag or coated with paint, wet samples and those subjected to heat treatment, and also
208 when a 1.5-metre NIR fibre-optic probe has been used.

209

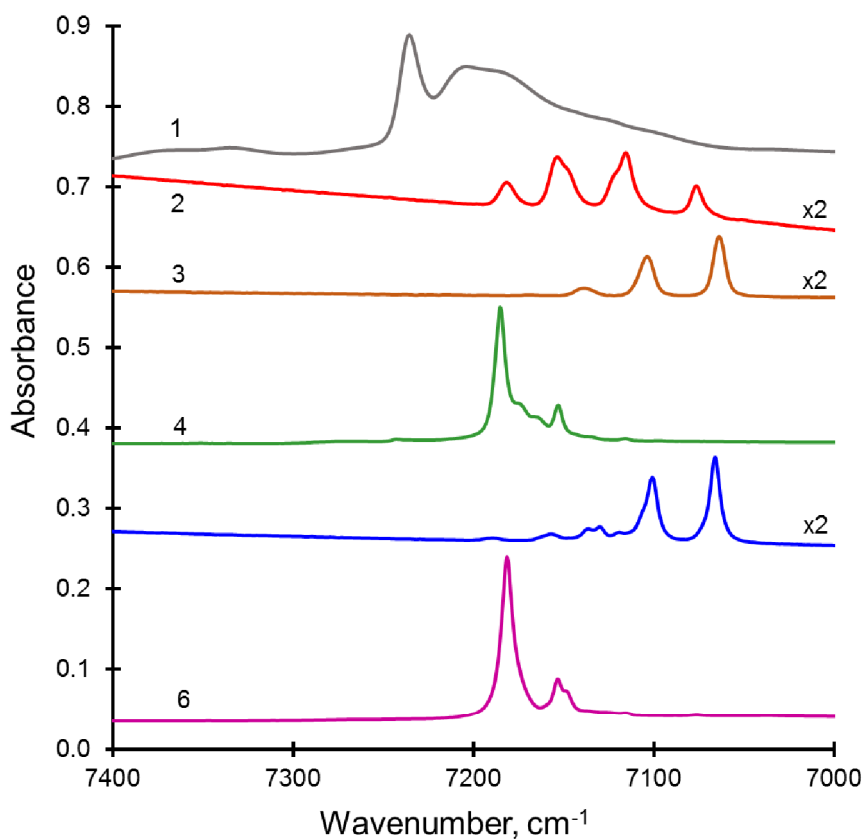


Figure 3. NIR spectra of asbestos samples: (1) ó chrysotile, (2) ó actinolite, (3) ó amosite, (4) ó anthophyllite, (5) ó crocidolite, (6) ó tremolite (resolution = 2 cm^{-1}).

210

211

212 Figures 4 and S11 present NIR spectra of amosite, crocidolite and chrysotile imbedded
 213 into different matrices at a range of concentration. The data show a high signal to noise ratio
 214 even for the samples with asbestos concentration of 0.1 wt%, making it evident that NIR spectra
 215 can be used for the detection of trace quantities of asbestos. In agreement with [19], the very
 216 high sensitivity of NIR spectroscopy in the overtone region of O-H vibrations can be explained
 217 by the very significant sampling depth (estimated as ~1 mm for NIR, as compared to ~10 μ for
 218 the mid-IR region) and the high values of the anharmonicity constants for these vibrations, which
 219 are summarised in Table 1 along with the OH band positions observed in the mid- and near-IR
 220 spectra.

221

222 Table 1. The positions of OH band, $(\text{O-H})_{0 \rightarrow 1}$ and $(\text{O-H})_{0 \rightarrow 2}$, and the values of the
 223 anharmonicity (χ_e) constant calculated for various O-H vibrations.

	$(\text{O-H})_{0 \rightarrow 1}, \text{cm}^{-1}$	$(\text{O-H})_{0 \rightarrow 2}, \text{cm}^{-1}$	ω_e, cm^{-1}	χ_e
Chrysotile	3700 (shoulder)	7236	3864	0.0212
	3683	7204	3842	0.0211
	3643			
Actinolite	3673	7182	3837	0.0214
	3659	7154	3823	0.0215
	3643	7116	3813	0.0223
		7076		
Amosite	3653	7136	3823	0.0222
	3637	7104	3807	0.0223
	3618	7064	3790	0.0227
Anthophyllite	3674	7185	3837	0.0212
	3658	7153	3821	0.0213
Crocidolite		7157		
	3650	7130	3820	0.0223
	3635	7101	3804	0.0222
	3619	7066	3791	0.0227
Tremolite	3674	7181	3841	0.0217
	3660	7153	3827	0.0218

224

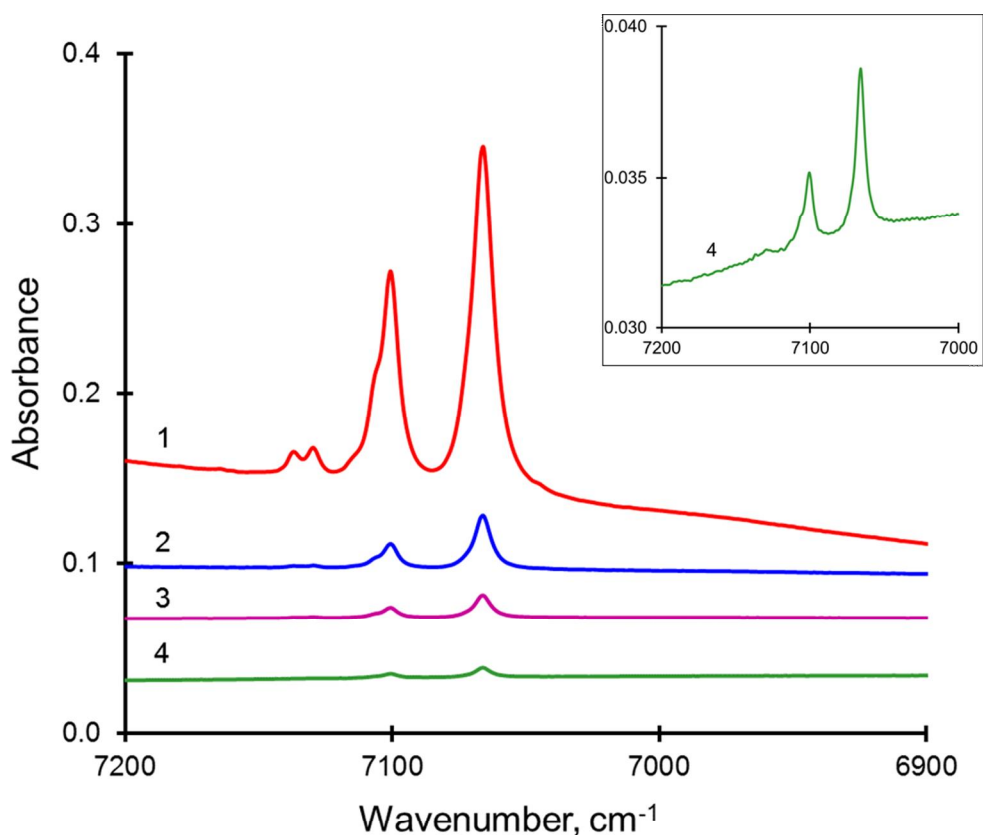


Figure 4. NIR spectra of crocidolite in CaCO₃: (1) 100%, (2) 10%, (3) 1%, (4) 0.1% (resolution = 2 cm⁻¹). Insert demonstrates the high signal to noise ratio in the NIR spectrum of the 0.1 wt% sample.

225

226 Figure S12 shows NIR spectra of most commonly found types of asbestos: chrysotile,
 227 amosite and crocidolite, as 1 wt% mixtures in calcium carbonate. For a combination of chrysotile
 228 with any amphibole, the identification of each component is straightforward, whereas the
 229 discrimination of amosite and crocidolite in their mixture is the most challenging task in
 230 spectroscopic analysis of asbestos. This can be successfully achieved if the data are collected at a
 231 high resolution, 2 or 4 cm⁻¹, in the region of 7300-7000 cm⁻¹ (Figure S12b). Moreover, careful
 232 deconvolution of the spectra would yield the fraction of each type of asbestos present. The value
 233 of high resolution data is highlighted by Figure S13, which presents NIR spectra of actinolite,
 234 amosite, crocidolite and chrysotile recorded at different spectral resolution. As it changes from 2
 235 to 32 cm⁻¹ (this corresponds to ~0.39 and ~6.2 nm), a significant amount of information is lost.
 236 For instance, the NIR spectra of amosite and crocidolite, which can be readily distinguished at 2
 237 cm⁻¹, become almost identical at the 32 cm⁻¹ resolution (Figure S13e). It should be noted that
 238 most wide-range NIR spectrometers, particularly portable and hyperspectral models that could
 239 be used for on-site and remote analysis, operate at a rather low resolution, 10 to 50 nm [26,27].
 240 Clearly, for a reliable real-world identification of asbestos, the NIR instrumentation should be
 241 capable of collecting the spectra at a high resolution in the 7300-7000 cm⁻¹ range.

242 For practical asbestos detection, it is essential to develop analytical procedures which
243 would be objective and could be readily automated. Therefore, we designed and tested a facile
244 computational algorithm for the analysis of NIR spectra obtained at a high resolution, 2 or 4 cm^{-1} ,
245 in the region of 7300-7000 cm^{-1} . The program has been evaluated using 50 samples with 9 data
246 sets for each sample (see Table S5). The results, computed for every data set utilising the
247 position and intensity of the bands observed in each NIR spectrum, indicate the presence or
248 absence of different types of asbestos. Table S6 presents a selection of the final outputs (a
249 complete set is included in SI as a csv file), which demonstrate notable agreement with all
250 available data for the composition of the questioned samples. Clearly, NIR spectra show high
251 sensitivity between 7300 and 7000 cm^{-1} ; focusing on this narrow region has the added advantage
252 of eliminating most undesirable contributions from various matrix components and contaminants,
253 while high resolution data facilitate excellent discrimination for all types of asbestos, making
254 NIR an effective and objective tool for the analysis of ACM.

255

256 ***Conclusions***

257 The following conclusions and recommendations result from this work:

- 258 1. FTIR spectroscopic studies using ATR sampling have demonstrated that asbestos can be
259 detected in a wide range of materials. Chrysotile, crocidolite, amosite, tremolite, anthophyllite
260 and actinolite show bands in the 3700-3500 cm^{-1} and 1200-500 cm^{-1} regions, which can be used
261 to identify asbestos in mixtures with many other materials. Some of these materials, however,
262 show bands in the same region as asbestos, and thus, can interfere with its detection. For instance,
263 absorption bands in the OH-region and in the region of structural vibrations are observed in the
264 infrared spectra of cement and inorganic fibres. Furthermore, in some ACM, asbestos fibres
265 appear to be completely coated with paint or bitumen preventing their identification. Therefore,
266 for samples with low asbestos concentration and for materials containing asbestos fibres fully
267 encapsulated within a polymer matrix, the FTIR results have been inconclusive. For the samples
268 with an unknown asbestos content, computational analysis provides a more confident
269 identification, but only in ACM with over 20 wt% of asbestos. It should be noted that ATR-FTIR
270 requires direct contact between the probe and the sample, whereas FTIR sampling in
271 transmittance mode using KBr disks would require additional lab-based sample preparation.
- 272 2. Raman spectroscopy is potentially very well suited to the in situ or on-site analyses, as the
273 spectra are not affected by the presence of water or container materials to any significant degree.
274 However, despite the initial expectations, it has not been found useful for the identification of
275 asbestos in ACM. The quality of the spectra has been poor, with low signal to noise ratio and
276 considerable fluorescence background. Using two laser sources improved the results for
277 reference samples providing more spectral information, however, asbestos identification has not

278 been possible in any of the studied building materials. It can also be expected that any impurity,
279 which is characterised by either strong Raman scattering or intense fluorescence, would nullify
280 any improvements achieved with this analytical technique.

281 3. NIR studies demonstrate that in the 7300-7000 cm^{-1} region, each type of asbestos has a
282 distinct pattern of absorption bands corresponding to the first overtone of the O-H stretching
283 vibrations. The remarkable sensitivity of this technique can be linked to the high anharmonicity
284 of the O-H vibrations and a substantial sampling depth. Furthermore, NIR does not require direct
285 contact between the probe and the sample, which can be therefore contained, avoiding asbestos
286 exposure. By focusing on the narrow spectral range and optimising the resolution level, each of
287 the six types of asbestos can be differentiated with the limit of detection as low as 0.1 wt%.
288 Furthermore, straightforward computational analysis has been used for an automated objective
289 processing of the spectroscopic data. The results of this work demonstrate that NIR spectroscopy
290 is potentially the most powerful technique for rapid, accurate and reliable detection and
291 identification of asbestos in real-life materials utilised by the construction industry.

292

293 **Acknowledgments**

294 The authors thank Keele University, Innovate UK and Greenwall Environmental for the funding
295 provided for this research. The authors are grateful to M. Wilks for providing ACM samples, Dr.
296 E. Garrett for technical assistance and Dr. R. Gertisser for helpful discussion and for providing
297 geological asbestos samples.

298 **CRedit authorship contribution statement**

299 VZ: supervision, methodology, data collection, data analysis, validation, writing - original draft,
300 review and editing. FR: supervision, methodology, writing - review and editing. AZ: software,
301 data analysis, validation, writing - review and editing. AH: data collection, data analysis, writing
302 - original draft, review and editing.

303 **Supplementary Information**

304 Supplementary data for this article can be found on-line at:

305

306 **Conflict of interest**

307 The authors declare no competing financial or any other interest.

308

References

- 1 M. Ross, A.M. Langer, G.L. Nord, R.P. Nolan, R.J. Lee, D. Van Orden, J. Addison. *The mineral nature of asbestos*, Regulatory Toxicology and Pharmacology, (2008), 52 (1), S26-S30.
- 2 S. Speil, J.P. Leineweber. *Asbestos minerals in modern technology*, Environmental Research, **1969**, 2, 166-208.
- 3 M.M. Morshed, A.S.M.A. Haseeb. *Physical and chemical characteristics of commercially available brake shoe lining materials: a comparative study*, Journal of Materials Processing Technology, **2004**, 155-156, 1422-1427.
- 4 C.L. Blake, G.S. Dotson, R.D. Harbison. *Assessment of airborne asbestos exposure during the servicing and handling of automobile asbestos-containing gaskets*, Regulatory Toxicology and Pharmacology, **2006**, 45 (2), 214-222.
- 5 Asbestos: The analysts' guide for sampling, analysis and clearance procedures, **2005**, Health and Safety Executive, UK.
- 6 A.F. Gualtieri, C. Cavenati, M. Meloni, G. Elmi, M. Lassinantti-Gualtieri. *The transformation sequence of cement–asbestos slates up to 1200°C and safe recycling of the reaction product in stoneware tile mixtures*, Journal of Hazardous Materials, **2008**, 152 (2), 563-570.
- 7 Health and Safety Laboratory MDHS 100. Surveying, sampling and assessment of asbestos containing materials **2001**, Health and Safety Executive, UK.
- 8 U.S. Geological Survey, 2020, Mineral commodity summaries, **2020** 26-27 <https://doi.org/10.3133/mcs2020>.
- 9 C.B. Manning, V. Vallyathan, B.T. Mossman. *Diseases caused by asbestos: mechanisms of injury and disease development*, International Immunopharmacology, **2002**, 2, 191-200.
- 10 R. Rudd. *Asbestos and the lung*, Medicine, **2004**, 36 (5), 261-264.
- 11 J. Gamble. *Risk of gastrointestinal cancers from inhalation and ingestion of asbestos*, Regulatory Toxicology and Pharmacology, **2008**, 52 (1), S124-S153.
- 12 K. Santee, P.F. Lott. *Asbestos analysis: a review*, Applied Spectroscopy Reviews, **2003**, 38, 355-394.
- 13 G. Wille, D. Lahondere, U. Schmidt, J. Duron, X. Bourrat. *Coupling SEM-EDS and confocal Raman-in-SEM imaging: A new method for identification and 3D morphology of asbestos-like fibers in a mineral matrix*, Journal of Hazardous Materials, **2019**, 374, 447-458.
- 14 R.P. Bagioni. *Separation of chrysotile asbestos from minerals that interfere with its infrared analysis*, Environmental Science and Technology, **1975**, 9, 262-263.
- 15 A. Marconi, *Application of infrared spectroscopy in asbestos mineral analysis*. Annali dell'Istituto Superiore di Satina. **1983**, 19, 629-638.
- 16 C. Rinaudo, E. Belluso, D. Gastaldi. *Assessment of the use of Raman spectroscopy for the determination of amphibole asbestos*, Mineralogical Magazine, **2004**, 68, 455-465.

- 17 D. Bard, J. Yarwood, B. Tylee. *Asbestos fibre identification by Raman microspectroscopy*, Journal of Raman Spectroscopy, **1997**, 28, 803-809.
- 18 E. Foresti, E. Fornero, I.G. Lesci, C. Rinaudo, T. Zuccheri, N. Roveri. *Asbestos health hazard: A spectroscopic study of synthetic geoinspired Fe-doped chrysotile*, Journal of Hazardous Materials, **2009**, 167, 1070-1079.
- 19 I.R. Lewis, N.C. Chaffin, M.E. Gunter, P.R. Griffiths. *Vibrational spectroscopic studies of asbestos and comparison of suitability for remote analysis*, Spectrochimica Acta A, (1996) 52, 315-328.
- 20 V. Sontevska, G. Jovanovski, P. Makreski. *Minerals from Macedonia. Part XIX. Vibrational spectroscopy as identificational tool for some sheet silicate minerals*. Journal of Molecular Structure, **2007**, 834-836, 318-327.
- 21 E. Foresti, M. Gazzano, A.F. Gualtieri, I.G. Lesci, B. Lunelli, G. Pecchini, E. Renna, N. Roveri. *Determination of low levels of free fibres of chrysotile in contaminated soils by X-ray diffraction and FTIR spectroscopy*. Analytical and Bioanalytical Chemistry, **2003**, 376, 653-658.
- 22 D. Bard, B. Tylee, K. Williams, J. Yarwood. *Use of a fibre-optic probe for the identification of asbestos fibres in bulk materials by Raman spectroscopy*, Journal of Raman Spectroscopy, **2004**, 35, 541-548.
- 23 C. Rinaudo, D. Gastaldi, E. Belluso. *Characterization of chrysotile, antigorite and lizardite by FT-Raman spectroscopy*, Canadian Mineralogist, **2003**, 41, 883-890.
- 24 J. R. Petriglieri, E. Salvioli-Mariani, L. Mantovani, M. Tribaudino, P. P. Lottici, C. Laporte-Magoni, D. Bersani. *Micro-Raman mapping of polymorphs of serpentine*, Journal of Raman Spectroscopy, **2015**, 46, 953-958.
- 25 J.W.Robinson, E.M.S.Frame. G.M. Frame, *Undergraduate Instrumental Analysis*, CRC Press, 2014, 313-321.
- 26 C. Bassani, R.M. Cavalli, F. Cavalcante, V. Cuomo, A. Palombo, S. Pascucci, S. Pignatti. *Deterioration status of asbestos-cement roofing sheets assessed by analyzing hyperspectral data*, Remote Sensing of Environment, **2007**, 109, 3616378.
- 27 G. Bonifazi, G. Capobianco, S. Serranti. *Asbestos containing materials detection and classification by the use of hyperspectral imaging*, Journal of Hazardous Materials, **2018**, 344, 981-993.